

Electrical properties and phase transitions of trimethylammonium-iodine-tetracyanoquinodimethane (TMA-I-TCNQ)

T. Ikari,* S. Jandl, and M. Aubin

Département de Physique, Université de Sherbrooke, Sherbrooke, Québec J1K 2R1, Canada

K. D. Truong

Département de Chimie, Université de Sherbrooke, Sherbrooke, Québec J1K 2R1, Canada

(Received 14 March 1983)

Temperature dependences of the resistivity and the anisotropic thermoelectric power of trimethylammonium-iodine-tetracyanoquinodimethane single crystals were measured. Two phase transitions at 150 and 82 K were confirmed by the transport measurements. Above 150 K, the transport properties are well interpreted in terms of an intrinsic semiconductor with a one-dimensional tight-binding band and a strong Coulomb interaction. The estimated band gap is 0.14 eV and the mobility ratio of electrons to holes is 0.8.

I. INTRODUCTION

The physical properties of quasi-one-dimensional molecular crystals have been studied extensively in recent years. Among these crystals, the ternary component material TMA-I-TCNQ (trimethylammonium-iodine-tetracyanoquinodimethane) is of particular interest giving rise to a controversy concerning the importance of the interaction between the two different chains (TCNQ and iodine).^{1,2} Although some initial results of the physical properties obtained from x-ray³ and optical⁴ measurements have been reported on this material, no thorough study of the electron transport properties has been carried out.

The crystal of TMA-I-TCNQ has a monoclinic structure with lattice parameters $a=20.35$ Å, $b=6.46$ Å, $c=13.92$ Å, and $\beta=115^\circ$.¹ The TCNQ molecules stack along the b axis (chain axis) with an interplanar distance of 3.23 Å, and the molecular plane is perpendicular to the b axis. The iodine atoms also form chains along the b axis with the same distance as that of TCNQ molecules. Filhol *et al.*³ have recently reported a one-dimensional superlattice ascribed to a periodic distortion on the iodine chain and a two-dimensional disorder of the iodine chains in the plane perpendicular to the b axis at room temperature.

This compound is well described as $(\text{TMA})^+(\text{I}_3^-)_{1/3}(\text{TCNQ})^{2/3-}$ with a $\frac{1}{3}$ -filled band on the TCNQ chains in the one-electron picture and it undergoes two phase transitions at 150 and 80 K.⁵ Although the transition at 150 K has been explained in terms of the Peierls-type metal-semiconductor¹ or semiconductor-semiconductor transition,⁵ the discussions are still a matter of controversy. As for the transition at 80 K, there is no direct evidence from electron transport measurements. The lack of experimental results so far may be due to an extremely high resistance of the samples near that temperature.

In this paper we report on the temperature dependences of the resistivity and the anisotropic thermoelectric power (TEP) of TMA-I-TCNQ from 60 to 400 K. The phase transition at 150 K is confirmed and the first direct evi-

dence for the phase transition at 82 K from transport measurements is also shown. The electrical properties above 150 K are analyzed in terms of a tight-binding band model with strong Coulomb interaction. Finally, we conclude that the TMA-I-TCNQ is a semiconductor above 150 K.

II. EXPERIMENTAL PROCEDURES AND RESULTS

Large single crystals of TMA-I-TCNQ were grown in the same way as that reported in Ref. 6. X-ray diffractometer measurements were carried out by using single crystals to characterize the material.

The dc resistivity measurements along the b axis were performed using a standard four-probe technique in the temperature range from 60 to 300 K. Good Ohmic contacts were obtained by evaporating gold onto the sample. Fine gold wires were mounted onto the gold electrode by using silver paint, being as careful as possible to avoid any stresses in the sample. The resistance of the sample at room temperature is about 10 Ω , and the current through the sample was maintained at a low level of about 1 μA . The resistance increased rapidly at a current greater than 100 μA . Around 70 K, the resistance of the sample reached $10^8 \Omega$.

Temperature dependences of the resistivity along the b axis are shown in Fig. 1, where the solid circles are in the cooling run and the crosses are in the subsequent heating run. The resistivity above 160 K sometimes jumps to higher values at nonreproducible temperatures. But below 160 K, no such behavior was observed. The data shown in Fig. 1 did not show the nonreproducible effects mentioned above. Since the interruption of the chain can easily halt the conduction entirely in a strand of a linear-chain material, the observed jump of the resistance may be due to such an interruption of the current path.

The resistivity of the sample is 0.18 $\Omega \text{ cm}$ at room temperature and increases gradually with decreasing temperature contrary to the sample measured by Brill *et al.*⁵ It begins to increase rapidly below about 160 K and then shows a kink at 80 K in the cooling run. There is also a kink at 85 K in the heating run, but the kink is smeared

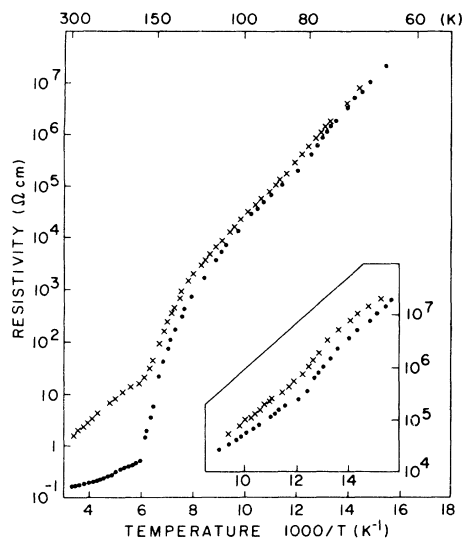


FIG. 1. Temperature dependences of the resistivity of the typical sample along the b axis in the cooling (solid circles) and the subsequent heating run (crosses). The results of another sample which show prominent kinks at 82 K are shown in the inset of the figure.

out. The results of another sample, which shows more prominent kinks at 82 K, are shown in the inset of the figure.

Although the resistivity at room temperature usually increased by a factor of 10 after the first temperature cycle, the increases of the resistivity became small and were within a few percent in the subsequent cooling and heating runs. The rapid changes at 160 K and the kinks at 82 K are reproducible. The estimated activation energy above 150 K is 0.07 eV in the heating run. The same activation energy was obtained for other single-crystal samples.

The TEP measurements give direct information about intrinsic properties of quasi-one-dimensional crystals. The TEP is independent of the sample geometry and is a zero-current phenomena. Therefore, an interruption of the current path does not produce a sizable effect unless there is also a large interruption in the heat-flow path.

The TEP of TMA-I-TCNQ along the b axis as well as that along the a axis was measured by using a slow ac technique such as that for the quasi-one-dimensional transition-metal trichalcogenides.⁷ Good results were obtained by using evaporated gold contacts. The absolute TEP of the sample was calculated by using the absolute TEP of pure gold metal.⁸ The TEP below 80 K could not be observed because of the extremely high resistance of the sample. Since the single crystals have a needlelike shape along the b axis, the TEP along the b axis (θ_b) is easily observed with great accuracy. For the TEP measurements perpendicular to the b axis (θ_a), the samples must be cut so that the a -axis dimension is larger than the b -axis dimension. The smallness of the samples gives rise to errors when measuring the temperature gradient. In order to estimate the accuracy of θ_a , we again measured θ_b by using a small sample with the same dimensions as for θ_a . The estimated uncertainty in θ_a was less than 20%.

Temperature dependences of θ_b and θ_a are shown in Fig. 2 by the solid circles and crosses, respectively. Note that the vertical scale is different below and above 150 K. At room temperature, θ_b is negative and has a value of $-27 \mu\text{V/K}$. The absolute value of θ_b decreases with decreasing temperature, crosses zero at around 170 K, and increases very suddenly below 150 K saturating to the value of about $-700 \mu\text{V/K}$ at around 90 K. The temperature dependence of θ_b above 150 K is well fitted by the equation

$$\theta_b = -\frac{k}{e} \left[0.67 - \frac{110 \text{ K}}{T} \right]. \quad (1)$$

The value of 110 K agrees with that reported by Brill *et al.*⁵ The fitted curve is shown by the solid line in the figure. The deviations of the experimental points from the curve above 350 K may be due to a degradation of the sample.⁹ All the samples show exactly the same temperature variation within the experimental error even when the sample undergoes many temperature cycles. Neither the hysteresis nor the nonreproducible discontinuity which appeared in the resistivity measurements were observed.

The TEP along the a axis (θ_a), perpendicular to the chain axis, has a positive value of $+18 \mu\text{V/K}$ at room temperature and increases with decreasing temperature. The temperature dependence above about 220 K can be fitted by

$$\theta_a = -\frac{k}{e} \left[0.22 - \frac{130 \text{ K}}{T} \right]. \quad (2)$$

The value of θ_a changes sign and increases negatively with a strong temperature dependence below 150 K. Since we could not evaporate the gold electrodes onto the sample in this configuration, no data were available below 120 K. The measurements for the different samples gave a value of θ_a constant within 10%.

III. DISCUSSION

Although there are two different types of chains in the crystal, it is usually assumed that only the TCNQ chains

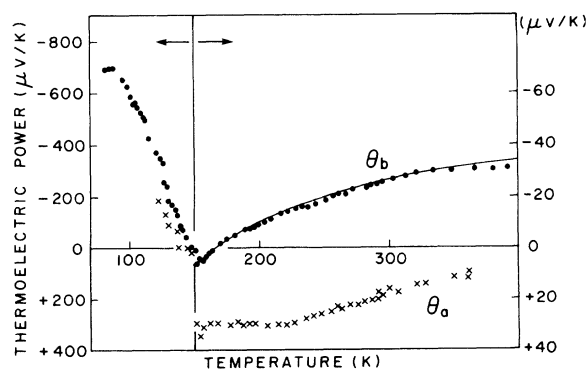


FIG. 2. Temperature dependence of the TEP along (θ_b) and perpendicular to the b axis (θ_a) are indicated by the solid circles and crosses, respectively. Note that the vertical scale is different below and above 150 K. The calculated curve is drawn by the solid line for θ_b .

can carry current.^{1,2} The iodine chains are considered as a perturbation to the TCNQ chains.

The phase transition at 150 K is confirmed by the sudden changes in the temperature dependences of the resistivity and the TEP, Figs. 1 and 2. Since it was not easy to determine the phase-transition temperature (T_c) from the resistivity measurement, T_c was determined more accurately to be 150 K from the TEP measurement. The phase transition at 150 K has been characterized in terms of the superlattice formation on the TCNQ chain with a periodicity of $3b$ along the b axis by neutron¹⁰ and high-voltage electron-diffraction measurements.¹¹ Since there is a $\frac{1}{3}$ -filled band in the TCNQ chain in the one-electron picture, the superlattice opens a gap at the Fermi level. Therefore, we can expect a gap in the density of states below the phase-transition temperature of 150 K. If the material is a metal above 150 K, this is the so-called Peierls transition.

Before discussing our results in the high-temperature phase above 150 K, we briefly review the two controversial explanations of the physical properties, one in terms of a semiconductor and the other in terms of a metal. Abkowitz *et al.*² have reported that the temperature dependence of the conductivity has a broad maximum near 240 K and decreases with increasing temperature above 240 K. The conductivity of their typical sample is $20 \Omega^{-1} \text{cm}^{-1}$ at room temperature. Assuming that the material is a semiconductor with a finite gap of 0.14 eV in the density of states, they explained the conductivity maximum as a product of the thermally activated carrier concentration and the strongly temperature-dependent mobility due to a significant coupling of electrons to a molecular vibrational mode of TCNQ.² The results of the room-temperature polarized reflectance measurements also show that there is a gap of 0.1–0.14 eV at 300 K.⁴ This gap would arise from a periodic potential on the TCNQ chains induced by the distortion on the iodine chain which has a periodicity of $(\frac{3}{2})b$.^{1,2} A different explanation has been proposed by Coulon *et al.*¹ and by Filhol *et al.*¹⁰ They assumed that the effect of the iodine chains is weak because of the disorder of the chains in the plane perpendicular to the b axis. Since the potential may be small when averaged over all the iodine chains, one would expect a metallic behavior above 150 K. However, their data, like ours, shows a decrease of the resistivity with increasing temperature above 150 K. They concluded that the semiconducting behavior originated from the interruption of the current path in the TCNQ strand.

Returning to our experimental results, the temperature dependence of the TEP above 150 K shows a semiconducting behavior with an activation energy of 110 K as shown in Fig. 2. We recall that this is a zero-current measurement and is not affected by the breaks in the TCNQ chains. The results of x-ray diffractometer measurements also suggest that the material is a semiconductor. We observed a very narrow and strong reflection signal in the plane perpendicular to the b axis. Since iodine atoms are the strongest x-ray scatterers, we can consider that the iodine chain is not disordered in that plane, contrary to the assumption of Coulon *et al.*¹ The potential due to the periodic distortion along the b axis of the iodine chain is

thus quite effective and the material shows a semiconducting behavior as suggested by Abkowitz *et al.*² Therefore, we will analyze the electrical properties of TMA-I-TCNQ in terms of a semiconductor above 150 K.

As in the case for (NMP)(TCNQ) [N-methylphenazinium (NMP)],¹² we assume that a band concept and a relaxation-time formalism are applicable to TMA-I-TCNQ. With the use of a tight-binding form of dispersion for both the one-dimensional conduction and valence bands, which are separated by the gap of 2Δ , the effective masses of electrons and holes at the band extrema are given as

$$m_e = \frac{2\hbar^2}{l^2 E_1}, \quad (3)$$

$$m_h = \frac{2\hbar^2}{l^2 E_2}, \quad (4)$$

respectively. Here l is the distance between the TCNQ molecules along the chain axis and E_1 and E_2 are the bandwidths of the conduction and valence bands, respectively.

The temperature dependence of the TEP above 150 K was well described by Eq. (1). The presence of a temperature-independent contribution of about $-60 \mu\text{V/K}$ suggests strong Coulomb correlations as discussed below. In this case the probability of occupation $f(E)$ of a state with energy E is given by

$$f(E) = \left[1 + \frac{1}{2} \exp \left(\frac{E - E_F}{kT} \right) \right]^{-1}, \quad (5)$$

where E_F is the Fermi energy and the factor of $\frac{1}{2}$ arises from the fact that the state may only be singly occupied due to the strong Coulomb repulsion.

Applying a nondegenerate Boltzmann limit to the carrier distribution statistics, the concentrations of the conduction-band electrons n_0 and the valence-band holes p_0 are given by

$$n_0 = \frac{2}{3} \frac{1}{lac \sin\beta} \left(\frac{kT}{\pi E_1} \right)^{1/2} \exp \left(-\frac{E_c - E_F}{kT} \right), \quad (6)$$

$$p_0 = \frac{2}{3} \frac{1}{lac \sin\beta} \frac{1}{4} \left(\frac{kT}{\pi E_2} \right)^{1/2} \exp \left(\frac{E_v - E_F}{kT} \right), \quad (7)$$

where a , c , and β are the lattice parameters and E_c and E_v are the energies of the conduction- and valence-band extrema, respectively. Since there are two TCNQ chains in the unit cell and the band is $\frac{1}{3}$ filled, a factor of $\frac{2}{3}$ appears in the equations. The factor of 4 which appears in Eq. (7) but not in Eq. (6) arises from the factor of $\frac{1}{2}$ in the distribution function (5).

When impurities are of negligible effect, the intrinsic carrier concentration n is given by

$$n = \frac{1}{3} \frac{1}{lac \sin\beta} \left(\frac{kT}{\pi} \right)^{1/2} \left(\frac{1}{E_1 E_2} \right)^{1/4} \exp \left(-\frac{\Delta}{kT} \right), \quad (8)$$

and the Fermi energy is at the intrinsic position

$$E_F = \frac{1}{2}(E_c + E_v) + \frac{1}{4}kT \ln \left[\frac{E_1}{E_2} \right] - kT \ln 2. \quad (9)$$

The total TEP when both electrons and holes are taken into account is given by

$$\theta = (\sigma_n \theta_n + \sigma_p \theta_p) / (\sigma_n + \sigma_p), \quad (10)$$

where σ_n and σ_p are the conductivities of electrons and holes, respectively. The individual-band TEP has the form

$$\theta_n = -\frac{k}{e} \left[A_n + \frac{E_c - E_F}{kT} \right], \quad (11)$$

$$\theta_p = \frac{k}{e} \left[A_p + \frac{E_F - E_v}{kT} \right]. \quad (12)$$

The values of A_n and A_p are related to the energy dependence of the carrier scattering for electrons and holes, respectively. With the use of the mobility ratio of $b = \mu_e / \mu_h$, where μ_e and μ_h are the mobilities of electrons and holes, respectively, Eq. (10) becomes

$$\theta = -\frac{k}{e} \left[\frac{b-1}{b+1} \frac{\Delta}{kT} + \ln 2 - \frac{1}{4} \ln \left[\frac{E_1}{E_2} \right] + \frac{bA_n - A_p}{b+1} \right]. \quad (13)$$

The constant value of $\ln 2$ arises from the factor of $\frac{1}{2}$ in Eq. (5) and is the same as that expected in a system with a large on-site Coulomb repulsion.¹³ Since the activation energy above 160 K is known ($\Delta = 0.07$ eV from Fig. 1), the mobility ratio b is calculated by the temperature-dependent terms of Eqs. (1) and (13) and is estimated at 0.8 assuming equal relaxation times for electrons and holes. With this assumption, the temperature-independent terms lead to estimates for the carrier scattering constants: $A_n = A_p = 0.7$. These values of A_n and A_p will be discussed below. The effective mass of electrons has been estimated at $6m_0$ from the optical measurements.⁴ With the use of this value along with our value of $b = 0.8$, the widths of the conduction E_1 and the valence band E_2 are estimated to be 0.24 and 0.32 eV, respectively, from Eqs. (3) and (4).

Since we can estimate the intrinsic carrier concentration n by Eq. (8), the temperature dependence of the Hall mobility is calculated for each sample by using the resistivity data. The results are well interpreted by a simple power law of $\mu_H \propto T^{-\alpha}$. The resistivity, the calculated Hall mobility at room temperature, and the exponent α for the typical samples are listed in Table I. The value of α is different from sample to sample and varies from 3.5 to 0.2 from the highest to the lowest mobility samples. We consider that the value of α reflects the sample quality. The carriers scattered by the interruption of the strand or imperfection may give rise to a small value of mobility including a temperature-independent contribution. Therefore, it is considered that the sample with $\alpha = 3.5$ is the purest one and gives an intrinsic behavior of the temperature variation. The observed exponent agrees with that of (NMP)(TCNQ), where α is about 4, and this strongly temperature-dependent mobility has been explained in terms of the interaction of electrons with molecular vibra-

TABLE I. The resistivity, the calculated Hall mobility at room temperature, and the exponent of the temperature variation of mobility $\mu_H \propto T^{-\alpha}$ for the typical samples. All data were calculated from the initial cooling run except 4, which was calculated from the subsequent heating run.

Sample no.	Resistivity (Ω cm)	Hall mobility μ_H ($\text{cm}^2/\text{V s}$)	α
1	0.071	2.6	3.5
2	0.18	1.1	2.9
3	0.36	0.51	2.3
4	1.49	0.12	~ 0.2
5	1.53	0.11	~ 0.2

tions.¹²

It is necessary to know the energy dependence of the carrier relaxation time τ to discuss the scattering constant A_n and A_p in Eq. (13). Conwell¹⁴ has calculated the explicit formula of τ for the TCNQ chain in TTF-TCNQ [tetrathiafulvalene (TTF)] in terms of a scattering of the carriers by optical phonons derived from the symmetric molecular vibrations. Applying Boltzmann statistics to her Eq. (1) in Ref. 14, one can find the energy dependence of the relaxation time as $\tau \propto E^{-1/2}$. In the one-dimensional tight-binding case, A_n and A_p are estimated to be 1 in the same way as that reported by Ikari *et al.*⁷ for the low-dimensional material of ZrSe_3 . The observed value of $A_n = A_p = 0.7$ agrees with the expected value of 1. This shows that the carriers may be scattered by the molecular vibrations in TMA-I-TCNQ. The increase of the resistivity at room temperature after the temperature cycle is understood by the interruption of the chain which makes the mobility low and temperature independent, as seen in Table I.

The Hall coefficient may be important in discussing the conduction mechanism of TMA-I-TCNQ. The Hall coefficient at room temperature is estimated to be $0.2 \text{ cm}^3/\text{C}$ from Eq. (8). This value is difficult to measure at low-current level, which is necessary to obtain reproducible results as discussed before.

In the high-temperature phase above 150 K, the transverse TEP (θ_a) exhibits a positive sign and a room-temperature value of $+18 \mu\text{V}/\text{K}$. Comparing the temperature dependences of θ_b and θ_a , Eqs. (1) and (2), respectively, the activation energy is not so different. This suggests that the scattering term in Eq. (13), i.e., the last term, must be considerably different for θ_b and θ_a . The experimental data in the whole temperature region above 150 K cannot be explained by a simple formula. Since the resistivity perpendicular to the b axis is 400 times larger than that parallel to the b axis,² other transport mechanisms such as hopping conduction must be considered in this direction.

The steep rise of the resistivity along the b axis was observed in the temperature region between 160 and 130 K. Below about 130 K, the resistivity shows an activation energy of 0.13 eV, which agrees with that reported by Filhol *et al.*¹⁰ The TEP along the b axis also changes drastically below 150 K and reaches the maximum value of $-700 \mu\text{V}/\text{K}$ around 90 K. A very large TEP, as high as $+850$

$\mu\text{V}/\text{K}$, has been observed in undoped polyacetylene and was understood by a dilute concentration of carriers which hop among a set of localized states.¹⁵ An alternative explanation of such high TEP is a large phonon drag process in a semiconductor. At present, we do not have any evidence for such mechanisms.

Below 150 K, θ_a changes to negative values and exhibits the same temperature dependence as θ_b . Such behavior may indicate that the interchain interactions between the TCNQ chains are more effective below the phase-transition temperature.¹

A kink at 82 K with a hysteresis of a few degrees is observed in the temperature dependence of the resistivity (Fig. 1). The smallness of the kink would correspond to a small change of the conduction mechanism along the b axis due to the phase transition. We could not observe any anomaly near 80 K in the TEP measurement.

Brill *et al.*⁵ characterized the anomaly at 90 K in the temperature dependences of Young's modulus and internal friction as a phase transition associated with a freezing out of methyl group rotations. Below 80 K, a superlattice formation with a periodicity of $6a$ along the a axis has been reported by Garnier and Ayroles¹¹ using a high-voltage electron-diffraction technique. Filhol *et al.*¹⁰ have reported a different explanation of the phase transition at 80–90 K, that is, the structural phase transition from monoclinic to triclinic with decreasing temperature due to the rotation of the TCNQ molecules. There are no definitive explanations of this phase transition at around 80 K at present. In any case, the physical properties change

mainly in the plane perpendicular to the b axis and no drastic effects on the electron conduction along the b axis are expected. Therefore, the anomaly of the resistivity along the b axis at 82 K is considerably smaller than that of the 150-K phase transition.

IV. CONCLUSION

The resistivity and TEP of TMA-I-TCNQ along the chain axis (b axis) as a function of temperature were measured and two phase transitions at 150 and 82 K were confirmed by the transport properties. The TEP perpendicular to the chain axis also indicates the phase transition at 150 K and shows a positive sign above 150 K contrary to that along the b axis.

In the high-temperature phase above 150 K the electric properties are well explained by the semiconductor model with a one-dimensional tight-binding band and a strong Coulomb interaction. The estimated gap is 0.14 eV and the mobility ratio of electrons to holes is 0.8. Strongly temperature-dependent mobility and the evaluation of the temperature-independent term of the TEP suggest that the carriers are dominantly scattered by the vibrations of the TCNQ molecules. The interruption of the chain makes the mobility low and temperature independent.

ACKNOWLEDGMENT

We would like to thank Professor L. G. Caron for his valuable discussions.

*Permanent address: Department of Physics, Kurume University, 1635 Mii-machi, Kurume 830, Japan.

¹C. Coulon, S. Flandrois, P. Delhaes, C. Hauw, and P. Dupuis, *Phys. Rev. B* **23**, 2850 (1981).

²M. A. Abkowitz, J. W. Brill, P. M. Chaikin, A. J. Epstein, M. F. Froix, C. H. Griffiths, W. Gunning, A. J. Heeger, W. A. Little, J. S. Miller, M. Novatny, D. B. Tanner, and M. L. Slade, *Ann. N.Y. Acad. Sci.* **313**, 459 (1978).

³Par A. Filhol, M. Rovira, C. Hauw, J. Gaultier, D. Chasseau, and P. Dupuis, *Acta Crystallogr. Sect. B* **35**, 1652 (1979).

⁴D. B. Tanner, J. E. Deis, A. J. Epstein, and J. S. Miller, *Solid State Commun.* **31**, 671 (1979).

⁵J. W. Brill, A. J. Epstein, and J. S. Miller, *Phys. Rev. B* **20**, 681 (1979).

⁶K. D. Truong, A. D. Bandrauk, C. Carlone, and S. Jandl, in *Proceedings of the International Conference on Low Dimensional*

Conductors, Les Arcs, France (1982) (unpublished).

⁷T. Ikari, R. Provencher, S. Jandl, and M. Aubin, *Solid State Commun.* **45**, 113 (1983).

⁸R. D. Barnrad, *Thermoelectricity of Metals and Alloys* (Taylor and Francis, London, 1972), p. 192.

⁹M. F. Froix, A. J. Epstein, and J. S. Miller, *Phys. Rev. B* **18**, 2046 (1978).

¹⁰A. Filhol, B. Gallois, J. Langier, P. Dupuis, and C. Coulon, *Mol. Cryst. Liq. Cryst.* **84**, 17 (1982).

¹¹T. Granier and R. Ayroles, *C. R. Acad. Sci.* **294**, 303 (1982).

¹²A. J. Epstein, E. M. Conwell, D. J. Sandman, and J. S. Miller, *Solid State Commun.* **23**, 355 (1977).

¹³J. F. Kwak and G. Beni, *Phys. Rev. B* **13**, 652 (1976).

¹⁴E. M. Conwell, *Phys. Rev. Lett.* **39**, 777 (1977).

¹⁵Y. W. Park, A. Denenstein, C. K. Chiang, A. J. Heeger, and A. G. MacDiarmid, *Solid State Commun.* **29**, 747 (1979).